Available online at www.sciencedirect.com
ScienceDirect
Acta Materialia 58 (2010) 5646–5653
Acta MATERIALIA
www.elsevier.com/locate/actamat

Measurement of grain boundary triple line energy in copper

B. Zhao [a], J.Ch. Verhasselt [b], L.S. Shvindlerman [a,c,d], G. Gottstein [a,*]

[a] Institut für Metallkunde und Metallphysik, RWTH Aachen University, 52056 Aachen, Germany
[b] Sparing Röhl Henseler, Rethelstr. 123, 40237 Düsseldorf, Germany
[c] Institute of Solid State Physics, Russian Academy of Sciences, Chernogolovka, Moscow District 142432, Russia
[d] State Technological University, Moscow Institute of Steel and Alloys, Russia

Received 18 November 2009; received in revised form 15 June 2010; accepted 19 June 2010
Available online 24 July 2010

Abstract

Recent studies have demonstrated that grain boundary triple junctions are crystal defects with specific thermodynamic and kinetic properties. In this study we address the energy of triple lines. Previously, a geometrical model was proposed to determine the grain boundary line tension. The current study introduces a thermodynamically correct approach which allows direct and precise measurement of the triple line energy. The experimental technique utilizes the measurement of the surface topography of a crystal in the vicinity of a triple junction by atomic force microscopy. The grain boundary triple line tension γ^{l}_{TP} of a random triple line in a copper tricrystal was measured to be $6.3 \pm 2.8 \times 10^{-9}$ J m^{-1}.

Keywords: Grain boundary; Triple junction; Line tension of boundary triple junction

1. Introduction

It was recognized recently that triple junctions are structural elements of a polycrystal with specific kinetic and thermodynamic properties, which can strongly impact microstructural evolution [1–3]. The effect of grain boundary junctions on recovery, recrystallization and grain growth, especially in fine-grained and nanocrystalline materials, opens up new opportunities to control and design the grain microstructure of polycrystalline aggregates.

The problem of triple line energy was discussed by Gibbs, who came to the conclusion that the excess free energy of a triple line between fluid phases might be positive or negative [4]. McLean [5] contended that triple junctions should have a positive energy owing to the influence of three connected grain boundaries.

The excess free energy of grain boundary junctions was studied by molecular dynamics (MD) by Srinivasan et al. [6], who concluded that a negative triple line energy is possible. Computer simulation studies performed by Van Swygenhoven [7] contradicted this conclusion: the triple line tension obtained was always positive. This contradiction was attributed to the linkage of grain size and grain boundary width, which was neglected in Ref. [6]. Nishimura [8] and Fortier et al. [9] assumed that the triple junction groove has the shape of a tetrahedron. Based on this hypothesis, the first experimental attempts were made to determine the triple line energy, and in one case a measurable line energy of at least 5×10^{-7} J m^{-1} was found. Using the same concept of measuring the pit depth at a triple junction to determine the triple line energy, Kim et al. [10], concluded from their results on nanocrystalline thin films of ZrO_2 that about 20% of the triple junctions in ZrO_2 exhibited a detectably elevated energy. However, they did not determine the triple line energy.

In fact, there is a poor body of the data to resolve this issue by properly conducted experiments, mainly due to both the experimental difficulties and the lack of a rigorous theoretical basis. The current investigation is

* Corresponding author.
E-mail address: Gottstein@imm.rwth-aachen.de (G. Gottstein).

1359-6454/$36.00 © 2010 Acta Materialia Inc. Published by Elsevier Ltd. All rights reserved.
doi:10.1016/j.actamat.2010.06.039

designed to resolve this controversy and render more reliable results.

2. Theoretical background

As outlined in the following theory section, our model does not impose the unrealistic constraint that the triple junction groove has the shape of a tetrahedron. By contrast, our measurements confirmed that the groove root is curved during its approach to the triple junction and only remains straight far away from the junction in accordance with the assumptions of our model. The geometry of our model is based on the thermal grooving of grain boundaries due to annealing.

The thermal grooving at grain boundaries which intersect the crystal surface has been used frequently to measure the surface tension of these grain boundaries relative to the energy of the two adjacent crystal surfaces. A typical thermal groove formed at a tilt grain boundary which intersects the free surface at 90° is shown in Fig. 1.

If the orientation of the surface on both sides of the grain boundary is the same and the root of the groove is straight, the specific grain boundary energy is given by:

$$\gamma_B = 2\gamma_S \cos\frac{\theta}{2} \tag{1}$$

where θ is the dihedral angle at the groove root under the assumption that the grain boundary is symmetric, and γ_B, γ_S are the grain boundary tension and the free surface tension, respectively.

In the case that the grain boundary remains flat but curved in the root of the groove (Fig. 2), one has to take into account an additional term, which is determined by the so-called line tension γ^{lS} of the grain boundary groove, i.e.

$$\gamma_B - \frac{\gamma^{lS}}{R} = 2\gamma_S \cos\frac{\xi}{2} \tag{2}$$

where R is the radius of curvature at the given point of the groove root. Eq. (2) can be rewritten as:

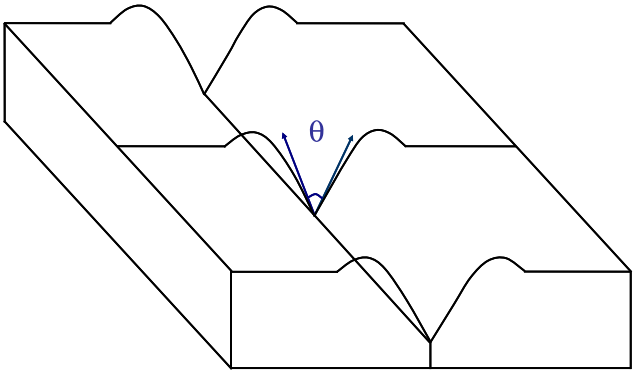

Fig. 1. Grain boundary groove formed at a straight, non-curved grain boundary with no variation in height.

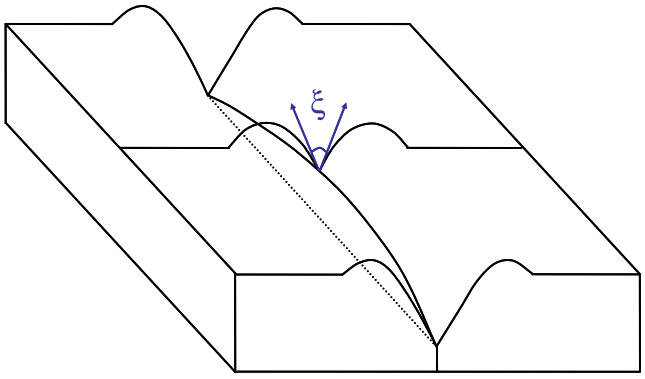

Fig. 2. Grain boundary formed at a flat grain boundary with a curved groove root.

$$\gamma_B - \gamma^{lS}\frac{\frac{\partial^2 u}{\partial r^2}}{\left[1+\left(\frac{\partial u}{\partial r}\right)^2\right]^{3/2}} = 2\gamma_S \cos\frac{\xi}{2} \tag{3}$$

since $\frac{1}{R} = \frac{\frac{\partial^2 u}{\partial r^2}}{\left[1+\left(\frac{\partial u}{\partial r}\right)^2\right]^{3/2}}$. The term $u(r)$ describes mathematically the profile of the groove root. The dihedral angle denoted by ξ has the same meaning as θ in Eq. (2) but may be significantly different in magnitude owing to the curvature. Combining Eqs. (1) and (2) yields the line tension of the bottom of the grain boundary groove, i.e. the grain boundary–free surface line tension:

$$\gamma^{lS} = 2\gamma_S\left(\cos\frac{\theta}{2} - \cos\frac{\xi}{2}\right)\cdot R \tag{4}$$

Obviously the influence of the grain boundary–free surface line tension on the dihedral angle rises with decreasing R.

The topography of a triple junction [11] after thermal annealing is formed by three grain boundaries which meet as shown schematically in Fig. 3. The three groove roots are curved towards the triple junction but remain straight far away from this point. If one associates a line tension with the triple line, an equilibrium of the four competing

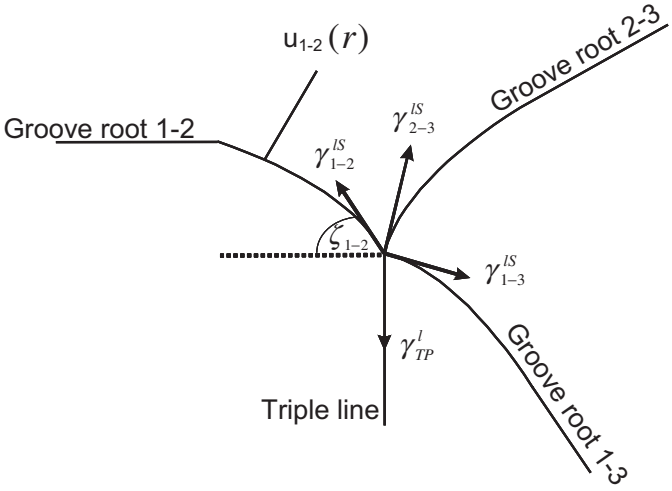

Fig. 3. Schematic 3D view of the line tension equilibrium at the triple junction.

line tensions (the three groove line tensions and the triple line tension) at the triple junction will be established. The three line tensions of the merging grain boundaries are denoted in Fig. 3 by γ^{IS}_{i-j}, where the indices i and j indicate the two grains on both sides of the grain boundary. From the equilibrium of the four line tensions it follows for the triple line tension:

$$\gamma^{l}_{TP} = \gamma^{IS}_{1-2}\sin\zeta_{1-2} + \gamma^{IS}_{1-3}\sin\zeta_{1-3} + \gamma^{IS}_{2-3}\sin\zeta_{2-3} \tag{5}$$

where ζ_{1-2}, ζ_{1-3} and ζ_{2-3} are the angles of each groove root of the corresponding grain boundary at the center of the triple junction. Therefore:

$$\sin\zeta_{i-j} = \sin\left(\arctan\left.\frac{\partial u_{i-j}}{\partial r}\right|_{r=0}\right) = \left.\frac{\frac{\partial u_{i-j}}{\partial r}}{\sqrt{1+\left(\frac{\partial u_{i-j}}{\partial r}\right)^2}}\right|_{r=0} \tag{6}$$

Eqs. (3)–(6) constitute the theoretical basis of the presented approach and can be used to calculate the triple line energy from the geometry of the merging boundaries at the triple junction.

The following requirements as dictated by Eqs. (1)–(6), and certain simplifying assumptions, are made in this study:

(1) The grain boundaries extend perpendicular to the crystal surface, i.e. at an angle of 90°.
(2) We neglect the so-called "torque terms" which account for the dependence of the grain boundary energy on boundary inclination. Therefore, we can determine the grain boundary energy for each grain boundary from Eq. (1), and thus reduce the number of parameters to the free surface energy and the dihedral angle.
(3) The surface tension γ_S of the crystal surfaces is independent of the surface orientation, and $\gamma_S = 1.75$ J m^{-2} under all experimental circumstances.
(4) We assume that the grain boundary–free surface line tension is constant along the grain boundary, and all three groove root line tensions γ^{l}_{i-j} are the same. Therefore Eq. (4) can be rewritten as:

$$\gamma^{l}_{TP} = \gamma^{IS}\cdot(\sin\zeta_{1-2} + \sin\zeta_{1-3} + \sin\zeta_{2-3}) \tag{7}$$

The first two simplifications will be ascertained during experiments, as the position of grain boundaries and the triple line will be checked, and the "torque terms" are negligible for random grain boundaries. Since the crystallography of the triple junction is not taken into account in this study, assumptions (3) and (4) are reasonable.

3. Experiments

A copper tricrystal was investigated to determine the triple line energy. The orientations of the crystals were measured by electron backscatter diffraction in a scanning electron microscope. The Euler angles of the three grain boundaries GB12, GB23 and GB31 were 31.51° $\langle\bar{1}\,4\,3\rangle$ (offset 2.05°), 52.86° $\langle 1\,\bar{4}\,4\rangle$ (offset 0.75°) and 32.93° $\langle 4\,\bar{1}\,0\rangle$ (offset 4.64°), respectively. These results indicate that none of the boundaries was a special grain boundary, i.e. low Σ coincidence boundary, or a low-angle grain boundary.

To ascertain that the grain boundaries and triple junctions were perpendicular to the surface, the tricrystal was sectioned perpendicular to the longitudinal specimen axis. Each section had lateral dimensions of around 1.5 cm^2 and a thickness of 2 mm. The samples were etched with nitric acid to reveal the location of the grain boundaries on both the top and bottom surface of the sample. Only samples where the grain boundaries and triple line were perpendicular to the surface were used for the measurements. They were ground with abrasive paper P1200, P2400 and P4000 and then mechanically polished with a water-based diamond suspensions of 3 and 1 μm.

To obtain a smooth surface, we used electropolishing with a method introduced by Verhasselt [12]. The specimens were electropolished at room temperature in a still electrolyte (274 ml 85% orthophosphoric acid + 66 ml distilled water). The low voltage of 1.75 V caused a slow electropolishing of at least 1 h, which guaranteed a high surface quality.

Finally, the specimens were placed in a vacuum furnace and annealed at high temperatures for different times. During the heat treatment thermal grooves developed, and for annealing times in excess of 1 h the development of grain boundary grooves could be observed by optical microscopy. The groove topography in close proximity to the triple junction was measured by atomic force microscopy (AFM).

Fig. 4 shows an example of groove formation at grain boundaries intersecting the crystal surface. The sample was annealed at 980 °C for 5 h. In the center of the figure there is a triple junction of the three adjoining grain boundaries (Fig. 4a).

The three grain boundary grooves meet at the triple junction, which extends as a triple line perpendicular to the surface (Fig. 4b). As shown schematically in Fig. 3, the three groove roots are curved in the vicinity of the triple junction but remain straight far away from this point.

A copper bicrystal with symmetrical 10° $\langle 1\,1\,0\rangle$ tilt grain boundary was used to measure the dihedral angle of the grain boundary groove, both for a straight and a curved grain boundary groove root. The samples were prepared the same way as explained above. The topography of the thermal groove is shown in Fig. 5.

4. Results

From the AFM measurements (Figs. 4 and 5) all necessary parameters can be derived to extract the triple line tension, such as the grain boundary groove angles, the groove root angles at the curved part of the grain boundary, and the curvature of the groove roots. To measure the dihedral

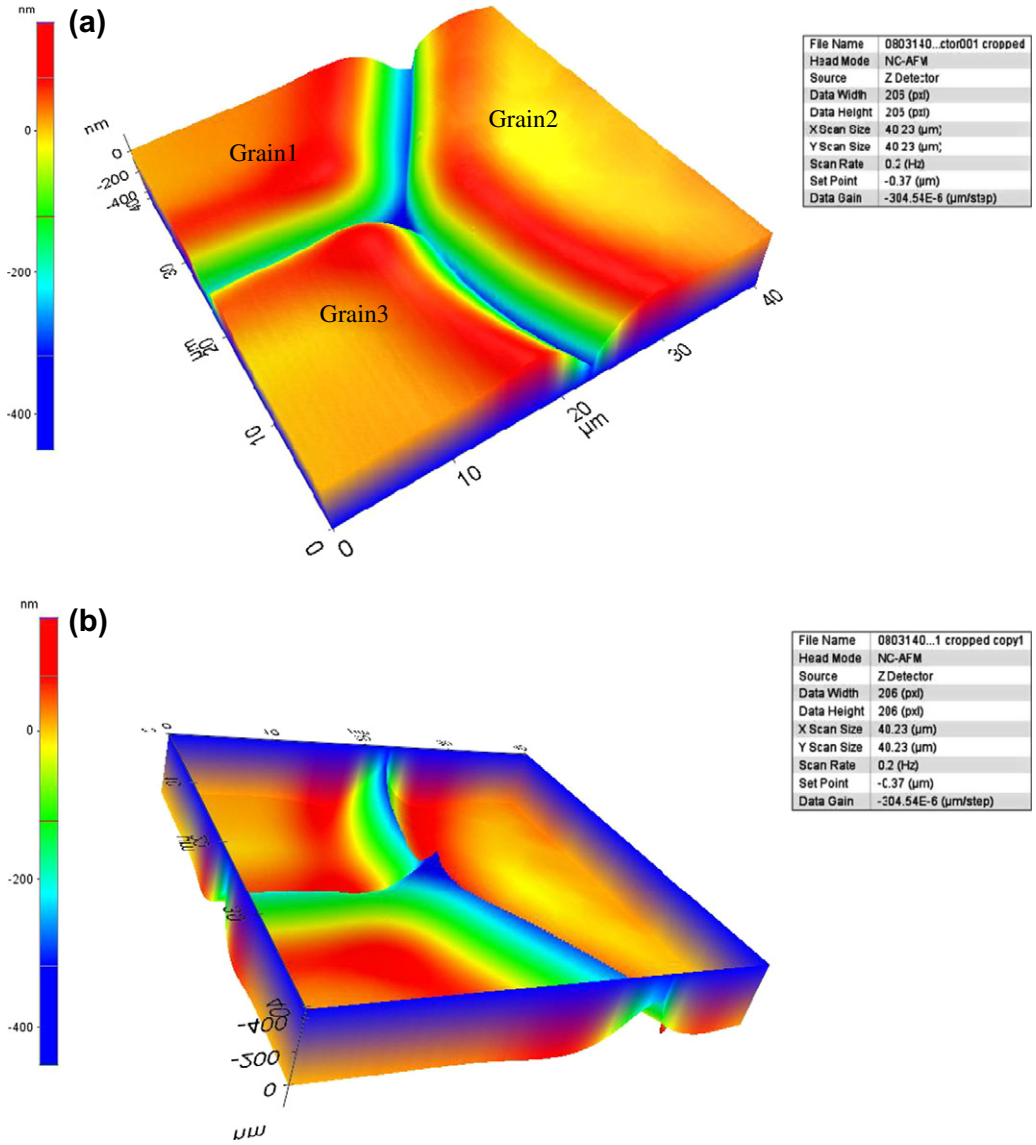

Fig. 4. Top view (a) and bottom view (b) of AFM topography measurement in the vicinity of a triple junction after annealing at 980 °C for 5 h. AFM image 40 μm × 40 μm, step size 0.19 μm.

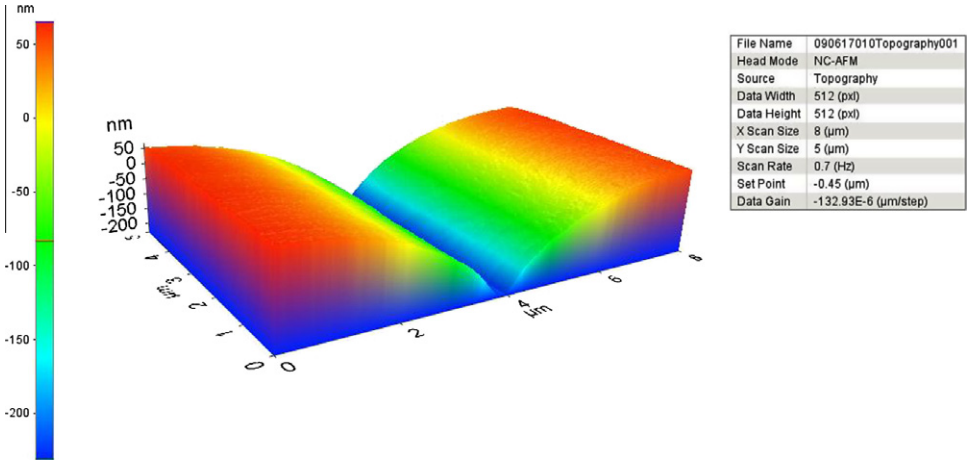

Fig. 5. Top view of AFM topography measurement on grain boundary groove of Cu bicrystal after annealing at 980 °C for 2 h. AFM image 8 μm × 5 μm, step size 16 nm along *X* and 10 nm along *Y*.

angles of the grain boundary grooves and therewith the grain boundary energy, we investigated the groove profiles perpendicular to the grain boundary in bicrystals (Fig. 6a).

The groove angle was measured on a plane perpendicular to the tangent of the groove root (tangent angle α in Fig. 6b). Owing to a large step size during the AFM scan, the exact location of the groove root and the dihedral angle right at the location of the groove root might be missed. To obtain this information, we fitted a shape function of a groove to the raw data, similar to the groove shape function derived by Mullins [13]:

$$y(x) = C_1 + C_2 \cdot x + C_3 \cdot x^2 \tag{8}$$

where C_1, C_2 and C_3 are constants for a given annealing time t. The square of the correlation coefficient was larger than 0.99, indicating an excellent fit.

Measured typical values for dihedral angles were in the range of 155°–164°, and the average of the grain boundary groove dihedral angle of a 10° ⟨1 1 0⟩ symmetrical tilt grain boundary was 161°, with a scatter of 2.3°.

The profiles of the groove roots were derived by examining the raw data of AFM images line by line. The points of the groove root were identified as the deepest points of the measured profile. To observe the influence of the grain boundary–free surface line tension on the dihedral angles, peaks in the groove root corresponding to a small radius of curvature were investigated to determine their radius and the respective dihedral angles. The profile in Fig. 6b shows that the radii of the three peaks along the groove root were 64 ± 15, 61 ± 12 and 59 ± 20 nm, and the corresponding dihedral angles at the peak positions had values of 150.2°, 152.5° and 152.4°, with a scatter of 2.3°. (It should

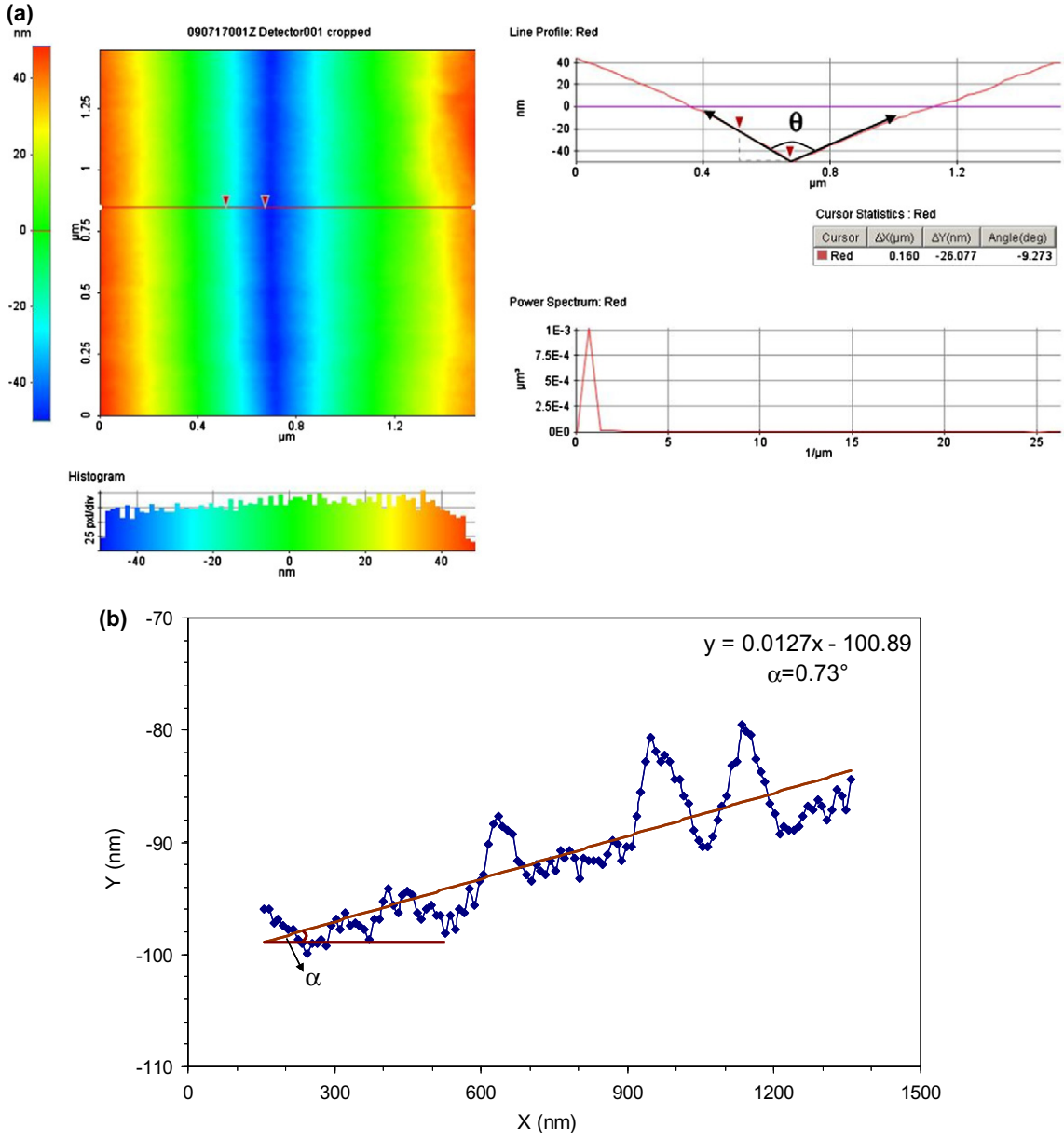

Fig. 6. (a) Profile perpendicular to the grain boundary grooves; (b) profile of the groove root.

be stressed that the equilibrium dihedral angle in copper is established rather rapidly [14].) The measured line tensions of the grain boundary groove root (triple line grain boundary–free surfaces) amount to $19.4 \pm 7.4 \times 10^{-9}$, $15.4 \pm 6.2 \times 10^{-9}$ and $15.5 \pm 7.3 \times 10^{-9}$ J m^{-1}, respectively, with an average value of $16.8 \pm 7.0 \times 10^{-9}$ J m^{-1}.

To derive the slope of the groove root at the triple junction, we measured the same area of a triple junction several times, and obtained the results $\zeta_{1-2} = 7.2° \pm 2.1°$, $\zeta_{2-3} = 7.6° \pm 2.1°$, $\zeta_{3-1} = 7.0° \pm 1.8°$.

If the energies of all three boundaries are independent of the grain boundary plane, the relation of the contact angle of three grain boundaries at a triple junction is given by the Young–Dupré equation [15]:

$$\frac{\gamma_{12}}{\sin\alpha_3} = \frac{\gamma_{23}}{\sin\alpha_1} = \frac{\gamma_{31}}{\sin\alpha_2} \tag{9}$$

The contact angles measured on the investigated tricrystal were 115.1°, 121.4° and 123.5°. The average variation of sinα was less than 5%, and was thus considered negligible.

Since the boundaries were not special grain boundaries or low-angle grain boundaries, we assumed the line tensions of the groove roots of all grain boundaries to be the same. With the mean value calculated above, the line tension of the specific triple line was $6.3 \pm 2.8 \times 10^{-9}$ J m^{-1}.

5. Discussion

5.1. Magnitude of triple line tension in Cu

According to our investigation on a Cu bicrystal and tricrystal, the measured triple line energy was $6.3 \pm 2.8 \times 10^{-9}$ J m^{-1}.

Our result is two orders of magnitude smaller than the experimental result of Fortier et al. [9]. This discrepancy must be attributed to different model assumptions. We assumed that the groove root is curved towards the triple junction and remains straight far away from this point, and this topographical feature was proved by AFM images (Fig. 4). With the hypothesis put forward by Fortier et al. [9] that the triple junction groove has the shape of a tetrahedron, the small triple line energy is not measurable. Therefore, of the four triple junctions characterized by Fortier et al.'s study, only one had a measurable line energy, which was at least 5×10^{-7} J m^{-1}, whereas the other three cases indicated that triple junctions had virtually negligible energies.

In the case that a triple line has the same spatial dimension as a dislocation with a line energy of about $\frac{1}{2}Gb^2$ [16], where G is the shear modulus and b is the Burgers vector, the triple line energy would be of the order of 10^{-9} J m^{-1}. Alternatively, a triple line can be considered as the intersection of three grain boundaries. In this case the energy of a triple line can be estimated as $\gamma^{l}_{TP} = \gamma_B \times \delta$, where δ is the grain boundary width. A corresponding simulation in Ref. [7] showed that the triple line energy in nickel samples was 1.41×10^{-9} J m^{-1}. The magnitude of our measured value agrees well with this assessment.

5.2. Accuracy of measurement

As the experimentally determined magnitude of the triple junction line tension depends sensitively on the angles ξ and θ and the curvature of the groove root at the triple junction, we conducted an error analysis to ascertain that the results and conclusions are reliable. The measurements were performed with high-aspect-ratio tips (OLYMPUS-AC11160BN-A2) in an atomic force microscope in non-

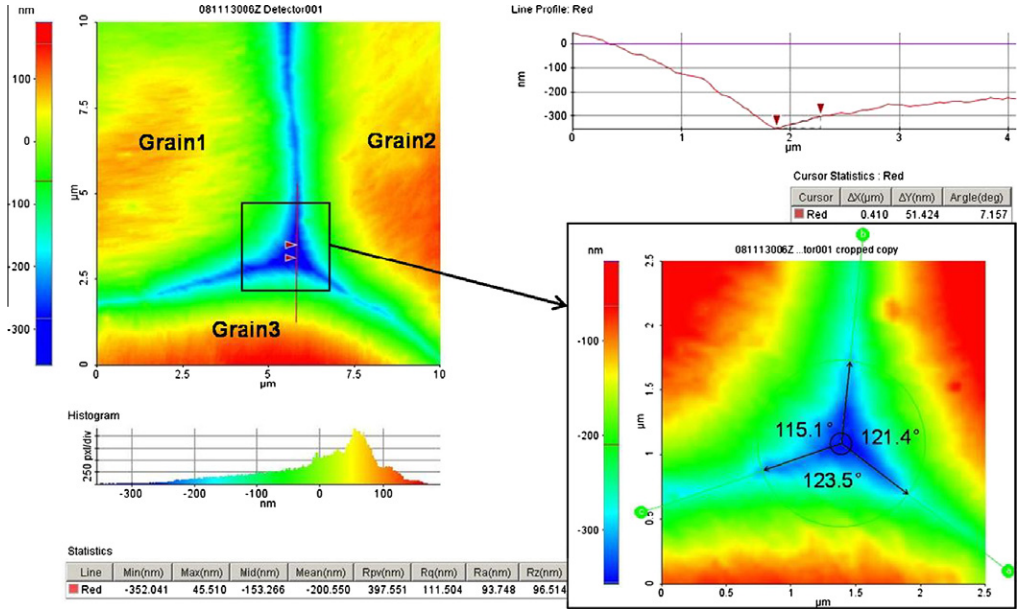

Fig. 7. Profile of the grain boundary grooves at the triple junction. AFM image 10 μm × 10 μm, step size 40 nm.

contact mode. The resolution of these tips was calibrated with a tip-check sample, and the geometry of the tip was derived by blind tip reconstruction. It rendered the information that the tip radius was about 10 nm with a slope of 72° (so a measurable dihedral angle must be larger than 36°). This allowed an accurate measurement of the triple junction geometry since the radius of curvature of the grain boundary groove roots was much larger, and the dihedral angles of grain boundary grooves were larger than 140°. Copper is liable to surface oxidation. However, the AFM measurements were conducted as soon as the samples were removed from the vacuum furnace. Therefore, although oxidation might have occurred, the thin oxide film would be essentially uniform, and would therefore not affect the magnitude and sign of the measured energy (see Fig. 7).

5.3. Positive or negative line tension

The sign of the triple line energy depends on the grain boundary–free surface energy, which is positive under equilibrium conditions. This is demonstrated as follows.

Let us assume that the profile of the grain boundary groove in a small region of length $2l$ can be described by the equation $y_1 = a_1x^2 + b_1$, with $a_1 = -b_1/l^2$, and the length of the grain boundary groove root is denoted by L_{root}. If the line tension of the grain boundary groove is negative, the root of the groove will tend to expand, and the corresponding elongated profile is $y_2 = a_2x^2 + b_2$, with $a_2 = -b_2/l^2$. The area of the grain boundary S_{GB} will increase, and the area change $\Delta S_{surface}$ of the connected two surfaces is composed of two parts. On the one hand, $S_{surface}$ will decrease by $\Delta S^b_{surface}$ due to the growing grain boundary area; on the other hand, $S_{surface}$ will increase by $\Delta S^r_{surface}$ because of the elongation of the groove root.

To derive the area change $\Delta S_{surface}$ of the connected two surfaces by the grain boundary, we need the profile of the grain boundary groove, which can be described by Eq. (8).

As the energy of the system

$$\Delta G = \gamma_S \cdot (\Delta S^b_{surface} + \Delta S^r_{surface}) + \gamma_{GB} \cdot \Delta S_{GB} + \gamma^{lS} \cdot \Delta L < 0 \tag{10}$$

the groove line can elongate by ΔL.

Since the radius of our tip is about 10 nm, we take $l = 100$ nm, $b_1 = 10$ nm, $R_{x=0} = 500$ nm. According to the measurement, the typical value of ξ is 161°, so the ratio of grain boundary energy to free surface energy is 0.33. From Eq. (10), -4.3×10^{-7} J m^{-1} is the largest value of the grain boundary–free surface line tension, and corresponds to the situation when the bottom of the groove root increases in height by one lattice constant 0.36 nm, i.e. from $b_1 = 10$ nm to $b_2 = 10.36$ nm. To decrease the energy of the total system the grain boundary–free surface line tension should be smaller than -4.3×10^{-7} J m^{-1}. In this case, the equilibrium dihedral angle ξ will attain 189° according to Eq. (4), which means that the interface of grain boundary and free surface will form a convex bulge which is higher than the surface (Fig. 8c), instead of a normal concave groove shape. Therefore a negative grain boundary–free surface line tension and the normal (classical) shape of thermal groove system cannot be in equilibrium. Since in our study the grain boundary–free surface line tension was measured in equilibrium, we have to conclude that the triple junction line tension must be positive.

6. Summary

We have proposed a thermodynamically correct approach for the determination of the energy of grain boundary triple lines. The corresponding measurements show that the line tension of random grain boundary triple junctions is positive and has the value $6.3 \pm 2.8 \times 10^{-9}$ J m^{-1}, whereas the grain boundary–free surface line tension is $16.8 \pm 7.0 \times 10^{-9}$ J m^{-1} on average. An accurate error analysis supports the determined magnitude of the measured triple line energy, and a detailed thermodynamic analysis

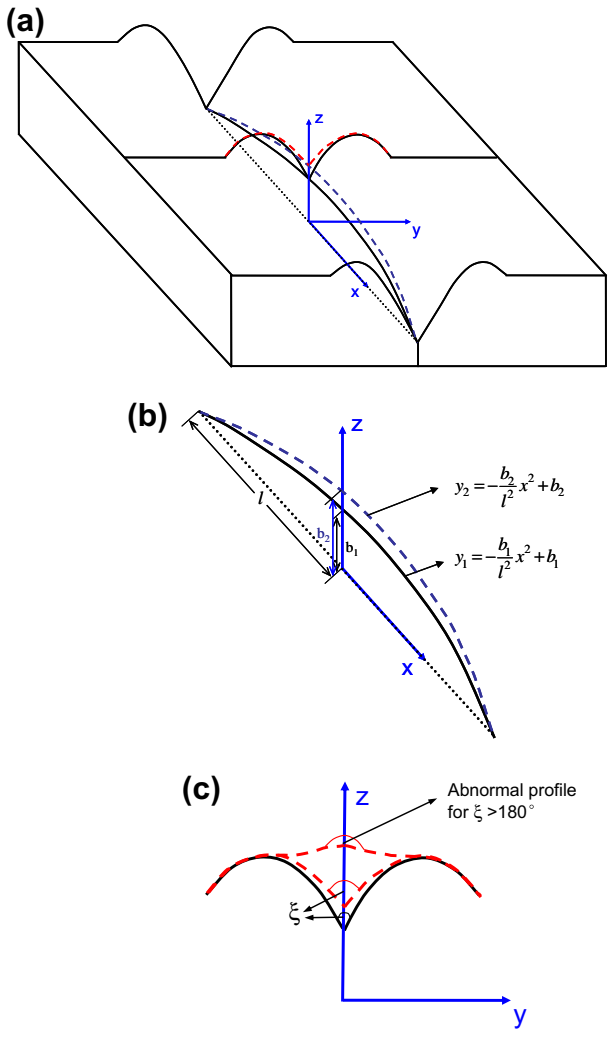

Fig. 8. (a) Schematic view of the free surface and grain boundary in 3D; (b) profile of grain boundary groove in the x–z plane; (c) profile of grain boundary groove in the x–y plane.

shows that the triple line and the grain boundary–free surface energy are positive under equilibrium conditions.

The current measurements were conducted on triple lines of random boundaries, and they disregarded triple junction crystallography, which will be subject of future investigations.

Acknowledgements

The financial support of the Deutsche Forschungsgemeinschaft (DFG) through project Go335/35-1 is gratefully acknowledged. We appreciate the financial support of the cooperation through the DFG Grant RUS113/846/0-2(R) and the Russian Foundation of Fundamental Research (Grant DFG-RRFI 09-02-91339).

References

[1] Czubayko U, Sursaeva VG, Gottstein G, Shvindlerman LS. Acta Mater 1998;46(16):5863–71.
[2] Gottstein G, Shvindlerman LS. Z Metallk 2004;95:219–22.
[3] Gottstein G, Shvindlerman LS. Scripta Mater 2005;52(9):863–6.
[4] Gibbs JW. Trans Connect Acad Arts Sci 1874;3:289.
[5] McLean D. Grain boundaries in metals. Oxford: Clarendon Press; 1957. p. 49.
[6] Srinivasan SG, Cahn JW, Jónsson H, Kalonji G. Acta Mater 1999;47:2821.
[7] Van Swygenhoven H. Phys Rev B 2001;63:134101.
[8] Nishimura G. M.A.Sc. Thesis. University of Toronto, 1973.
[9] Fortier P, Palumbo G, Bruce GD, Miller WA, Aust KT. Scripta Metall 1991;25:177.
[10] Kim H, Xuan Y, Ye PD, Narayanan R, King AH. Acta Mater 2009;57:3662.
[11] Galina AV, Fradkov VE, Shvindlerman Fiz LS. Khim Mekh Pov (Soviet Phys Chem Mech Surf) 1988;1:100.
[12] Verhasselt J. PhD thesis, RWTH-Aachen University, 2001.
[13] Mullins WW. J Appl Phys 1957;28(N3):333.
[14] Gjostein NA, Rhines FN. Acta Metall 1959;7(N3):224.
[15] Gottstein G. Physical foundations of materials science. Berlin: Springer; 2004. p. 106.
[16] Gottstein G. Physical foundations of materials science. Berlin: Springer; 2004. p. 234.